Centrum Rzeczoznawstwa Budowlanego

Inżynieria Bezpieczeństwa
Obiektów Antropogenicznych 3 (2024) 98-110
https://inzynieriabezpieczenstwa.com.pl/

Inżynieria Bezpieczeństwa Obiektów Antropogenicznych

Load-bearing capacity of single and multi-anchor connections – theory vs results of experimental research (part 1)

Dariusz TOMASZEWICZ [1], Krzysztof CZECH [2],
Jerzy K. SZLENDAK [3], Adam BARYŁKA [4*]

[1] *International Academy of Applied Sciences in Lomza, Poland*

[2] *Bialystok University of Technology, Bialystok, Poland*

[3] *Prof. Edward F. Szczepanik State Professional University Polytechnic Department in Suwalki, Poland*

[4] *Warsaw University of Life Sciences, Warsaw, Poland*

Abstract

The manuscript reviews the methods and mathematical relationships for estimating the theoretical load capacity of steel anchors – both single-anchor (bonded perpendicularly and diagonally to the surface) and multi-anchor systems. Input data for comparative analyses (experimental load capacity of anchors) were obtained from laboratory tests. A total of 62 R-STUDS bonded anchors, made from metric studding M12 threaded rods, made of carbon steel class 5.8, were tested. The scope of the tests included: 22 single anchors bonded at an angle of 90° to the concrete surface, 12 single diagonal anchors (4 anchors at 30°, 45° and 60° each), 16 anchors in twin-anchor systems at 30° and 45° angles, and 12 anchors in three-anchor systems (2 diagonal anchors at an angle of 60° and one at an angle of 90°). Laboratory tests, with the use of the HYSDOZOK hydraulic load-setting system, were carried out at Bialystok University of Technology in three stages. Comparison of the actual anchor load capacities (experimental load capacities) with the corresponding theoretical load capacities in each of the tested anchor groups showed very large discrepancies in the results (from -97.2% to +139.5%). Most of the results obtained indicate higher values of theoretical anchor load capacity (Pult) than experimental load capacity (Pexp). Further work on adjusting the mathematical relationships used to estimate the load capacity of steel anchors was needed. However, due to limitations in the size of the current manuscript, the results of work related to the application of heuristic algorithms to optimize the mathematical models will be presented in the authors' next publication.

Keywords: steel bonded anchors, theoretical and experimental anchor load capacity, comparative analysis

* **Corresponding author:** E-mail address: (adam_barylka@sggw.edu.pl) Adam Baryłka

https://dx.doi.org/10.37105/iboa.224
Received 01 August 2024
Available online 01 October 2024
ISSN 2450-1859, eISSN 2450-8721
Published by Centrum Rzeczoznawstwa Budowlanego

1 Introduction

Bonded anchors are the most frequently chosen element connecting the texture layer with the structural layer in the walls of three-layer large slab panel buildings. This is due to the nature of how they work in concrete (they do not cause additional stresses, compared with e.g. mechanical anchors). The theoretical estimation of the load-bearing capacity of bonded anchors can be made using the component method [1], which was originally used to calculate the load capacity and stiffness of steel and composite connections, and then adapted to connections with bonded anchors. It takes into account three parameters: anchor diameter d, effective anchor depth h_{ef} and adhesion stress τ_p. In the case of steel anchors embedded in concrete, the parameter that most significantly affects the load capacity is adhesion.

The first attempts to study and describe the phenomenon of adhesion of steel to concrete were made at the beginning of the 20th century. Pioneers in this field were Grabowski (1908) [2] and Bryła (1937) [3]. The latest results of research on the adhesion of steel to concrete can be found in the publication by Cruz-Sena et al. (2009) [4].

The choice of a method for testing the adhesion of steel to concrete should depend on whether the external surface of the anchors is smooth, ribbed or threaded. A loss of adhesion is possible:

- at the resin – steel anchor interface;
- or at the resin – concrete interface.

In order to estimate the load-bearing capacity of bonded anchors using the component method [1], it is necessary to determine the limit stresses of adhesion of steel to concrete f_{bd} [5], [6]. According to [6], these can be elastic, elastic-brittle, or plastic stresses. The size of the limit adhesion stresses is influenced by adhesion, by friction of steel against concrete caused by concrete shrinkage, and by meshing caused by uneven steel surface structure.

Adhesion stress between the steel anchor and the concrete or resin (at the contact zone) can be determined, according to Figure 1, from the equilibrium of forces in the system:

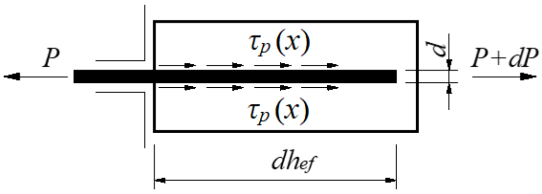

Figure 1. *Model of force distribution in the case of a single-anchor system* [6], [7]

$$-P - \tau_{adh}(x) \cdot u \cdot dh_{ef} + P + dP = 0, \quad (1)$$

where: P – tensile / pull-out force of the anchor [N, kN],

dP – increase in tensile (pull-out) force of the anchor [N, kN],

d – steel anchor diameter [mm],

$\tau_{adh}(x)$ – adhesion stress [N/mm^2]

dh_{ef} – increase in the effective anchorage length [mm],

$u = \pi \cdot d$ – anchor perimeter [mm].

Transforming equation (1) we obtain the increase in the tensile (pull-out) force in the anchor:

$$dP = \tau_{adh}(x) \cdot u \cdot dh_{ef}, \quad (2)$$

and adhesion stress:

$$\tau_{adh}(x) = \frac{dP}{u \cdot dh_{ef}}, \quad (3)$$

The magnitude of the limit adhesion stress depends on the shape of the steel anchor in addition to the strength of the resin and concrete [8].

The increase in the pull-out force of a steel anchor with a circular cross-section can also be written as a function of the stress increment:

$$dP = \frac{\pi \cdot d^2}{4} \cdot d\sigma_P. \quad (4)$$

At the same time, the adhesion stress takes the following form:

$$\tau_{adh}(x) = \frac{\pi \cdot d^2}{4} \cdot d\sigma_P \cdot \frac{1}{u \cdot dh_{ef}} = \frac{\pi \cdot d^2}{4} \cdot d\sigma_P \cdot \frac{1}{\pi \cdot d \cdot dh_{ef}} = \frac{d}{4} \cdot \frac{d\sigma_P}{dh_{ef}}. \quad (5)$$

Integrating equation (2) on both sides, we obtain the value of the anchor pull-out force over the effective anchorage length:

$$P = u \cdot \int_0^{h_{ef}} \tau_{adh}(x)dx \cdot h_{ef} = \pi \cdot d \cdot h_{ef} \cdot \int_0^{h_{ef}} \tau_{adh}(x)dx. \quad (6)$$

Anchorage can be destroyed by tensile forces and/or shear forces. In the case of tensile forces, failure can occur as a result of breakage of the anchor pin, the anchor being pulled out (loss of adhesion at the resin – steel anchor connection or loss of adhesion at the resin – concrete connection) or pulling out (breakage) of the concrete cone. In the case of excessive shear forces, however, the anchor bolt may be cut off, or the concrete edge may be broken and destroyed by prying.

As part of the study, an attempt was made to improve the existing mathematical relationships on the load-bearing capacity of bonded steel anchors. The input data required for the analysis (load-bearing capacity of the bonded steel anchors) were determined experimentally. In the simple models, it is assumed that the ultimate pull-out resistance of the anchor depends only on tensile force *P*. In the composite models, the ultimate load-bearing capacity of the anchored connection depends on tensile force *P*, shear force *V* (corresponding to the dead weight of the façade texture layer-of three-layer walls) and fastening factor a_M, which takes different values for anchoring only in the structural layer and different values for anchorage through all layers.

In order to improve the mathematical models, heuristic algorithms were used: genetic and local searches.

Optimizing the solution was about finding global extremes. The algorithms were validated by searching for local extremes using test functions.

Unfortunately, due to the extensiveness of the material, including the theoretical part, the obtained research results, mathematical modeling, and the optimization and validation of new mathematical models, it is impossible to present the whole study within one article. Therefore, the publication has been divided into two articles.

In the first article, the theory and methodology of determining the load-bearing capacity of single anchors (bonded perpendicularly and diagonally) and the load-bearing capacity of anchor groups (twin-anchor and three-anchor systems) is presented, as well as the results of the experimental tests. The first article ends with conclusions resulting from the comparison of the experimental load-bearing capacity with the theoretical load-bearing capacity of anchors. The second article will present the heuristic algorithms used by the authors to improve the mathematical models, as well as their optimization and validation.

2 Forms of anchor failure – estimation of load capacity

The basic form of destruction under consideration is **single anchor pull out**. The value of the pull-out force P_{ult} of the anchor can be estimated using the following equations:

$$P_{ult} = \pi \cdot d \cdot h_{ef} \cdot \tau_{adh-anchor} \quad \text{lub} \quad P_{ult} = \pi \cdot d_o \cdot h_{ef} \cdot \tau_{adh-concrete} \quad (7)$$

where: h_{ef} – effective anchorage length [*mm*],

d – the diameter of the anchor taken into account in the above-mentioned equation in the case of anchor pull-out at the junction of the resin and the steel anchor [*mm*],

d_o – diameter of the hole at the junction of resin and concrete [*mm*],

$\tau_{adh-anchor}$ – adhesion stress in the resin-steel anchor contact zone [N/mm^2],

$\tau_{adh-concrete}$ – adhesion stress in the resin-concrete contact zone [*N/mm*^{2}].

In the case of three-layer elements, the possibility of anchor pull-out as a result of the interaction of tensile force *P* and shear force *V* (determined as the dead weight of the concrete texture layer acting on a single anchor) should also be taken into account. In this case, the load-bearing capacity of the anchor should be determined using relationships [9], [10]:

$$P_{ult} = \sqrt{\left(\pi \cdot d \cdot h_{ef} \cdot \tau_{adh-anchor}\right)^2 + \left(\frac{V}{\alpha_M}\right)^2} \qquad (8)$$

$$P_{ult} = \sqrt{\left(\pi \cdot d_o \cdot h_{ef} \cdot \tau_{adh-concrete}\right)^2 + \left(\frac{V}{\alpha_M}\right)^2} \qquad (9)$$

where:

V – shear force corresponding to the dead weight of the concrete texture layer per anchor [*kN*],

α_M – anchor attachment factor, adopted in accordance with [11] (α_M = 1.0 in the absence of restraint when there is a possibility of free rotation; α_M = 2.0 in the case of full restraint when there is no free rotation and the anchor is restrained to the workpiece to be fastened by means of a washer and nut).

Another form of destruction of a single anchor is **concrete cone breakout failure**. In this case, the load-bearing capacity of the anchor should be determined using the following relation:

$$P_{ult} = \pi \cdot \left(r + \frac{d}{2}\right) \cdot \left(\sqrt{\left(r + \frac{d}{2}\right)^{\mathbf{2}} + h_{ef}^2}\right) \cdot f_{ctm} \qquad (10)$$

where: $r + \frac{d}{2}$ – cone radius [*mm*],

f_{ctm} – tensile strength of concrete [*N/mm*^{2}].

In concrete cone breakout failure, the anchorage capacity depends on the tensile strength of the concrete f_{ctm}, which is a function of the compressive strength of concrete. According to Model Code [12] and EC2 [13] , the tensile strength of concrete can be determined from relationship (11) and Table 3.1 of EC2 [13]:

$$f_{ctm} = 0.3 \cdot f_{ck}^{2/3} \qquad (11)$$

Taking into account, as before, the interaction of tensile force *P* with shear force *V*, we get:

$$P_{ult} = \sqrt{\left(\pi \cdot \left(r + \frac{d}{2}\right) \cdot \left(\sqrt{\left(r + \frac{d}{2}\right)^2 + h_{ef}^2}\right) \cdot f_{ctm}\right)^2 + \left(\frac{V}{\alpha_M}\right)^2} \qquad (12)$$

where: V / α_M – force taking into account the influence of shear force of the top texture layer [-].

The estimation of the load-bearing capacity of **single diagonal anchors** in the event of failure of the resin-steel anchor junction and the resin-concrete junction is carried out using the following formulas:

$$\boldsymbol{P_{ult} = \pi \cdot d \int_0^{h_{ef}} \tau_p} \mathrm{dx} \rightarrow \boldsymbol{P_{ult} = \pi \cdot d \cdot \tau_{adh-anchor} \cdot \frac{h_{ef}}{cos\alpha_k}}, \qquad (13)$$

$$\boldsymbol{P_{ult} = \pi \cdot d_o \int_0^{h_{ef}} \tau_p} \mathrm{dx} \rightarrow \boldsymbol{P_{ult} = \pi \cdot d_o \cdot \tau_{adh-concrete} \cdot \frac{h_{ef}}{cos\alpha_k}}. \qquad (14)$$

where: $cos\alpha_k$ – cosine of the angle of inclination of a single diagonal anchor [°].

The tensile strength of a concrete cone for a single diagonal steel anchor can be determined from the formula:

$$P_{ult} = \pi \cdot \left(r + \frac{d}{2}\right) \cdot \left(\sqrt{\left(r + \frac{d}{2}\right)^2 + \left(\frac{h_{ef}}{\cos\alpha_k}\right)^2}\right) \cdot f_{ctm}. \tag{15}$$

The load-bearing capacity formulas of single diagonal anchors (due to the lack of possibility of implementing such a solution in experimental tests) do not take into account shear force *V*.

For **complex two-** and **three-anchor systems**, the load capacity of the anchor group is determined using the relationship below. The emergence of these relationships was preceded by a number of tests and analyses [14]. The load-bearing capacity of the group of pull-out anchors and the load-bearing capacity of the anchor group damaged by concrete cone breakout failure should be estimated independently.

Load-bearing capacity of **pull-out two-anchor systems** are determined using formulas (16)-(19):

- damage to the anchorage due to anchor pull-out at the junction between the resin and the steel anchor

$$P^L_{ult1} = P_{1ult} + \frac{1}{2} \cdot \frac{V}{\alpha_M} \cdot \cos\alpha = \pi \cdot d \cdot \tau_{adhesive-anchor} \cdot \frac{h_{ef}}{\cos\alpha} + \frac{1}{2} \cdot \frac{V}{\alpha_M} \cdot \cos\alpha, \tag{16}$$

$$P^P_{ult2} = P_{2ult} - \frac{1}{2} \cdot \frac{V}{\alpha_M} \cdot \cos\alpha = \pi \cdot d \cdot \tau_{adhesive-anchor} \cdot \frac{h_{ef}}{\cos\alpha} - \frac{1}{2} \cdot \frac{V}{\alpha_M} \cdot \cos\alpha, \tag{17}$$

- damage to the anchorage due to anchor pull-out at the junction between the resin and the concrete

$$P^L_{ult1} = P_{1ult} + \frac{1}{2} \cdot \frac{V}{\alpha_M} \cdot \cos\alpha = \pi \cdot d_o \cdot \tau_{adhesive-concrete} \cdot \frac{h_{ef}}{\cos\alpha} + \frac{1}{2} \cdot \frac{V}{\alpha_M} \cdot \cos\alpha, \tag{18}$$

$$P^P_{ult2} = P_{2ult} - \frac{1}{2} \cdot \frac{V}{\alpha_M} \cdot \cos\alpha = \pi \cdot d_o \cdot \tau_{adhesive-concrete} \cdot \frac{h_{ef}}{\cos\alpha} - \frac{1}{2} \cdot \frac{V}{\alpha_M} \cdot \cos\alpha, \tag{19}$$

where: P^L_{ult1}, P^P_{ult2} – design ultimate load-bearing capacity of anchor connection breakage (on the left and right, respectively) [*kN*],

P_{1ult}, P_{2ult} – values of the pull-out load-bearing capacity of anchors without taking into account the influence of shear force load from the textured layer *V* [*kN*],

$\cos\alpha$ – cosine of the angle of inclination of single anchors [°].

In **three-anchor systems**, in addition to the two 60° diagonal anchors, an additional 90° anchor is used. The load-bearing capacity of such an anchor is determined according to formulas (20)-(21):

$$P_{ult1} = \sqrt{\left(P_{1gr}\right)^2 + \left(\frac{V}{\alpha_M}\right)^2} = \sqrt{\left(\pi \cdot d \cdot \tau_{adhesive-anchor} \cdot h_{ef}\right)^2 + \left(\frac{V}{\alpha_M}\right)^2}, \tag{20}$$

$$P_{ult2} = \sqrt{\left(P_{1gr}\right)^2 + \left(\frac{V}{\alpha_M}\right)^2} = \sqrt{\left(\pi \cdot d_o \cdot \tau_{adhesive-concrete} \cdot h_{ef}\right)^2 + \left(\frac{V}{\alpha_M}\right)^2}. \tag{21}$$

Load capacity of 60° bonded diagonal anchors (P^L_{gr2} and P^P_{gr3}) should be determined from (16)-(19).

The load-bearing capacity of **a group of anchors destroyed as a result of concrete cone breakout failure** is determined depending on the angle at which the damage occurred (30°, 45° or 60°).

If concrete cone breakout failure occurred at an angle of 30°, equations (22)-(23) were applied:

$$P^L_{ult1} = \frac{P_{1ult} \cdot A_{pb}}{\chi \cdot c \cdot l_{ef1}} + \frac{1}{2} \cdot \frac{V}{\alpha_M} \cdot \cos\alpha = \frac{\left(\pi \cdot \left(r + \frac{d}{2}\right) \cdot \left(\sqrt{\left(r + \frac{d}{2}\right)^2 + {h_{ef}}^2}\right) \cdot f_{ctm}\right) \cdot (c' + s) \cdot (c_3 + s_3)}{\chi \cdot c \cdot l_{ef1}} + \frac{1}{2} \cdot \frac{V}{\alpha_M} \cdot \cos\alpha, \tag{22}$$

$$P_{ult2}^{P}=\frac{P_{2ult}\cdot A_{pb}}{\chi\cdot c\cdot l_{ef2}}-\frac{1}{2}\cdot\frac{V}{\alpha_M}\cdot\cos\alpha=\frac{\left(\pi\cdot\left(r+\frac{d}{2}\right)\cdot\left(\sqrt{\left(r+\frac{d}{2}\right)^2+h_{ef}{}^2}\right)\cdot f_{ctm}\right)\cdot(c'+s)\cdot(c_3+s_3)}{\chi\cdot c\cdot l_{ef2}}-\frac{1}{2}\cdot\frac{V}{\alpha_M}\cdot\cos\alpha.\quad(23)$$

In the case of concrete cone breakout failure at an angle of 45°, equations (24)-(25) were applied accordingly:

$$P_{ult1}^{L}=\frac{P_{1ult}\cdot A_{pb}}{\chi\cdot c\cdot l_{ef1}}+\frac{1}{2}\cdot\frac{V}{\alpha_M}\cdot\cos\alpha=\frac{\left(\pi\cdot\left(r+\frac{d}{2}\right)\cdot\left(\sqrt{\left(r+\frac{d}{2}\right)^2+\left(h_{ef}\cdot\cos\alpha_1\right)^2}\right)\cdot f_{ctm}\right)\cdot(c'+s)\cdot c_3}{\chi\cdot c\cdot l_{ef1}}+\frac{1}{2}\cdot\frac{V}{\alpha_M}\cdot\cos\alpha,\quad(24)$$

$$P_{ult2}^{P}=\frac{P_{2ult}\cdot A_{pb}}{\chi\cdot c\cdot l_{ef2}}-\frac{1}{2}\cdot\frac{V}{\alpha_M}\cdot\cos\alpha=\frac{\left(\pi\cdot\left(r+\frac{d}{2}\right)\cdot\left(\sqrt{\left(r+\frac{d}{2}\right)^2+\left(h_{ef}\cdot\cos\alpha_1\right)^2}\right)\cdot f_{ctm}\right)\cdot(c'+s)\cdot c_3}{\chi\cdot c\cdot l_{ef2}}-\frac{1}{2}\cdot\frac{V}{\alpha_M}\cdot\cos\alpha.\quad(25)$$

When the angle at which the concrete cone breakout failure occurred was 60°, the load capacity of the anchor group was determined from equations (26)-(28):

$$P_{ult1}=\frac{P_{1ult}\cdot A_{pb}}{\chi\cdot c\cdot l_{ef,1}}+\frac{V}{\alpha_M}=\frac{\left(\pi\cdot\left(r+\frac{d}{2}\right)\cdot\left(\sqrt{\left(r+\frac{d}{2}\right)^2+h_{ef}{}^2}\right)\cdot f_{ctm}\right)\cdot(c'+s)\cdot c_3}{\chi\cdot c\cdot l_{ef,1}}+\frac{V}{\alpha_M},\quad(26)$$

$$P_{ult2}^{L}=\frac{P_{2ult}\cdot A_{pb}}{\chi\cdot c\cdot l_{ef,3}}+\frac{1}{2}\cdot\frac{V}{\alpha_M}\cdot\cos\alpha=\frac{\left(\pi\cdot\left(r+\frac{d}{2}\right)\cdot\left(\sqrt{\left(r+\frac{d}{2}\right)^2+\left(h_{ef}\cdot\cos\alpha\right)^2}\right)\cdot f_{ctm}\right)\cdot(c'+s)\cdot c_3}{\chi\cdot c\cdot l_{ef,3}}+\frac{1}{2}\cdot\frac{V}{\alpha_M}\cdot\cos\alpha,\quad(27)$$

$$P_{ult3}^{P}=\frac{P_{3ult}\cdot A_{pb}}{\chi\cdot c\cdot l_{ef,3}}-\frac{1}{2}\cdot\frac{V}{\alpha_M}\cdot\cos\alpha=\frac{\left(\pi\cdot\left(r+\frac{d}{2}\right)\cdot\left(\sqrt{\left(r+\frac{d}{2}\right)^2+\left(h_{ef}\cdot\cos\alpha\right)^2}\right)\cdot f_{ctm}\right)\cdot(c'+s)\cdot c_3}{\chi\cdot c\cdot l_{ef,3}}-\frac{1}{2}\cdot\frac{V}{\alpha_M}\cdot\cos\alpha.\quad(28)$$

Additional parameters were introduced to the above equations:

A_{pb} – surface area of the concrete element [mm^2],

χ – empirical proportionality coefficient [-],

c – thickness of the resin layer [mm],

l_{ef1}, l_{ef2} – total anchorage depth [mm],

c', s, c_3, s_3 – axial anchor spacing [mm].

The radius of the cone ($r + d / 2$) can be determined from the following relation:

$$\left(r+\frac{d}{2}\right)=h_{ef}\cdot\tan\alpha.\quad(29)$$

The empirical proportionality factor χ depends on the values of forces ratio P_{exp} / P_{exp1} and P_{exp} / P_{exp2}:

$$\chi=\frac{P_{exp}}{P_{exp1}}\cdot m\quad\text{oraz}\quad\chi=\frac{P_{exp}}{P_{exp2}}\cdot m,\quad(30)$$

where: P_{exp} – value obtained from experimental tests for single diagonal anchors bonded at angles of 30°, 45° and 60° [kN],

P_{exp1} i P_{exp2} – values obtained from experimental tests [kN],

m – multiplier depending on anchoring conditions [-].

In the case when: $\frac{P_{exp}}{P_{exp1}}>1.0$ and $\frac{P_{exp}}{P_{exp2}}>1.0$ – the value of the empirical proportionality coefficient is taken as for the fundamental conditions and denoted as χ_n (respectively χ_{n1} and χ_{n2}). The value of the multiplier m should then be determined from equations (31)-(32), which take into account the different strength parameters of the resin:

- at higher adhesion stresses (limit value approx.12 N/mm^2)

$$m_{wp} = \frac{t_{w,\min}^{20°C}}{t_{m,\min}^{10°C}}, \tag{31}$$

- with reduced adhesion stresses (limit value approx. 6 N/mm^2)

$$m_{mp} = \frac{t_{w,\min}^{15°C}}{t_{m,\min}^{15°C}}, \tag{32}$$

where: $t_{w,\,min}$ – minimum setting time [*min*],

$t_{m,\,min}$ – minimum assembly time [*min*].

In the case when: $\frac{P_{exp}}{P_{exp1}} < 1.0$ and $\frac{P_{exp}}{P_{exp2}} < 1.0$ – the value of the empirical proportionality coefficient is assumed for *unfavorable conditions* and denoted as χn (χ_{n1} and χ_{n2}, respectively). In this case, the value of multiplier *m* should be determined from the relation:

- at higher adhesion stresses (limit value approx. 12 N/mm^2)

$$m_{wn} = \frac{t_{w,\min}^{5°C}}{t_{m,\min}^{-10°C}}, \tag{33}$$

- with reduced adhesion stresses (limit value approx. 6 N/mm^2)

$$m_{mn} = \frac{t_{w,\min}^{5°C}}{t_{m,\min}^{-5°C}}. \tag{34}$$

Mixed conditions can apply: $\frac{P_{exp}}{P_{exp1}} < 1.0$ and $\frac{P_{exp}}{P_{exp2}} > 1.0$, or $\frac{P_{exp}}{P_{exp1}} > 1.0$ and $\frac{P_{exp}}{P_{exp2}} < 1.0$.

In such a case, the multipliers of the empirical coefficient are selected alternately.

3 Research results

For the purposes of this study, sixty-two metric screw anchors of type *R-STUDS* with *M*12 threaded rods of carbon steel class 5.8, were tested. This included 22 single anchors bonded in at an angle of 90° to the concrete surface, 12 single diagonal anchors (4 anchors at 30°, 45° and 60° each), 16 anchors in twin-anchor systems at 30° and 45° angles and 12 anchors in three -anchor systems (2 diagonal anchors at 60° and one at 90°).

The tests were carried out in three stages using a hydraulic load system (*HYSDOZOK*).

In the experimental tests carried out, not all forms of destruction mentioned in the previous section were observed. With bonded anchors in elements of small thickness, the anchor bolt does not break. There was also no case of concrete splitting, no destruction of the anchor connection by prying or shearing of the anchor bolt (this effect can only be caused by a bending load on the anchor).

The theoretical load-bearing capacity was calculated by analyzing the model (ideal) anchorage failure mechanism, in which the most important factors are the adhesion stress τ_p and the effective anchorage depth h_{ef}. The *experimental load-bearing capacity* was obtained from the experimental tests carried out, and also took into account other factors not included in the theoretical formulas.

In this work, in the calculation of the theoretical load-bearing capacity, approximate values of adhesion stresses determined during the shearing of resin samples with dimensions of 11 × 1 × 100 *mm* were assumed. In order to obtain more accurate values, additional tests of resin-to-concrete adhesion stresses and resin-to-steel adhesion stresses would need to be performed.

Table 1 presents the theoretical and experimental load-bearing capacity for twenty-two anchors bonded at an angle of 90° to the sample surface. The theoretical resistance was determined according to equations (8), (9) i (12).

Table 1. *Load-bearing capacity of single anchors bonded at* an angle of 90° *to the sample surface*

Anchor No.	Total anchorage length l_{ef} [*mm*]	Effective anchorage length h_{ef} [*mm*]	Theoretical load-bearing capacity P_{ult} [*kN*]	Experimental load-bearing capacity P_{exp} [*kN*]	$P_{ult} - P_{exp}$ [*kN*]	$(P_{ult} - P_{exp})/P_{ult}$ [%]
1	130	20	5.98	8.4	-2.42	-40.5
2	130	20	5.98	5.7	0.28	4.7
3	130	20	12.59	3.9	8.69	69.0
4	130	20	12.59	6.0	6.59	52.3
5	140	30	8.92	9.1	-0.18	-2.0
6	140	30	8.92	11.5	-2.58	-28.9
7	140	30	18.86	7.5	11.36	60.2
8	140	30	18.86	6.4	12.46	66.1
9	145	35	10.39	9.1	1.29	12.4
10	145	35	21.82	6.2	15.80	71.8
11	145	35	17.13	12.0	5.13	29.9
12	145	35	21.82	20.5	1.32	6.0
13	150	40	11.87	4.4	7.47	62.9
14	150	40	11.87	5.0	6.87	57.9
15	150	40	25.13	8.5	16.63	66.2
16	150	40	25.13	6.2	18.93	75.3
17	160	50	14.82	35.5	-20.68	-139.5
18	160	50	14.82	8.1	6.72	45.3
19	160	50	31.41	8.8	22.61	72.0
20	160	50	31.41	7.9	23.51	74.8
21	170	60	17.78	10.5	7.28	40.9
22	170	60	37.69	7.9	29.79	79.0

Anchors numbered 2, 4, 8-10, 12, 14-15, 18, 20 and 22 were bonded into three-layer concrete specimens made of C 12/15 concrete, while anchor numbers 1, 3, 5-7, 11, 13, 16-17, 19 and 21 were bonded into three-layer concrete specimens made of C 30/37 concrete. For anchor numbers 3-4, 7-8, 10-12, 15-16, 19-20 and 22, *Sika Anchor Fix-1* resin with average adhesion stress τ_p = 12.40 N/mm^2 was used in experimental tests. Anchor numbers 1-2, 5-6, 9, 13-

14, 17-18 and 21 use *R-KER Bonded Anchor* resin with average adhesion stress τ_p = 5.89 N/mm^2. In order to increase the readability of the results obtained, Table 1 highlights the numbers of anchors in which resin with more than twice the adhesion stress value was used. Similarly, the numbers of samples in which a higher class of concrete was used (C 30/37) are distinguished by **bold**.

Table 2 lists the load-bearing capacity results for single diagonal anchors. The theoretical load-bearing capacity of the anchors was determined according to relationships (13)-(15).

Table 2. *Load-bearing capacity of single diagonal anchors*

Anchor No.	Total anchorage length l_{ef} [mm]	Effective anchorage length h_{ef} [mm]	Theoretical load-bearing capacity P_{ult} [kN]	Experimental load-bearing capacity P_{exp} [kN]	$P_{ult} – P_{exp}$ [kN]	$(P_{ult} - P_{exp})/P_{ult}$ [%]
Single diagonal anchorages at an angle of 30° to the specimen surface						
1	95	80	17.75	11.9	5.85	33.0
2	95	80	37.68	10.6	27.08	71.9
3	95	80	17.75	17.8	-0.05	-0.3
4	95	80	37.68	30.5	7.18	19.1
Single diagonal anchorages at an angle of 45° to the specimen surface						
5	195	40	18.69	3.5	15.19	81.3
6	195	40	8.88	1.7	7.18	80.9
7	195	40	18.69	4.2	14.49	77.5
8	195	40	8.88	1.3	7.58	85.4
Single diagonal anchorages at an angle of 60° to the specimen surface						
9	165	35	10.36	11.2	-0.84	-8.1
10	165	35	21.80	0.6	21.20	97.2
11	165	35	21.80	9.1	12.70	58.3
12	165	35	10.36	2.9	7.46	72.0

The theoretical and experimental load-bearing capacities of the two-anchor systems are listed in Table 3. The theoretical load-bearing capacities were determined according to relationships (15)-(18) and (21)-(24).

Table 3. *Load-bearing capacity of two-anchor systems*

Anchor No.	Total anchorage length l_{ef} [mm]	Effective anchorage length h_{ef} [mm]	Theoretical load-bearing capacity P_{ult} [kN]	Experimental load-bearing capacity P_{exp} [kN]	$P_{ult} - P_{exp}$ [kN]	$(P_{ult} - P_{exp})/P_{ult}$ [%]
Diagonal anchorages – at an angle of 30° to the surface of the specimens						
1-L	290	72	34.01	2.5	31.51	92.6
2-R	290	72	33.27	9.7	23.57	70.8
3-L	290	72	34.01	4.9	29.11	85.6
4-R	290	72	33.27	9.0	24.27	72.9
5-L	290	72	25.85	17.7	8.15	31.5
6-R	290	72	15.61	6.1	9.51	60.9
7-L	290	72	16.35	3.2	13.15	80.4
8-R	290	72	15.61	1.0	14.61	93.6
Diagonal anchorages – at an angle of 45° to the surface of the specimens						
9-L	195	27	12.92	5.9	7.02	54.3
10-R	195	27	12.31	7.9	4.41	35.8
11-L	195	27	12.92	6.3	6.62	51.2
12-R	195	27	12.31	5.4	6.91	56.1
13-L	195	27	6.29	5.1	1.19	18.9
14-R	195	27	5.69	6.6	-0.91	-16.0
15-L	195	27	8.29	7.7	0.59	7.1
16-R	195	27	7.69	9.2	-1.51	-19.6

Table 4 lists the load-bearing capacities of three-anchor systems. Their theoretical load capacity was determined using the relationships (15)-(20) and (25)-(27).

Table 4. *Load capacity of three-anchor systems*

Anchor No.	Total anchorage length l_{ef} [*mm*]	Effective anchorage length h_{ef} [*mm*]	Theoretical load-bearing capacity P_{ult} [*kN*]	Experimental load-bearing capacity P_{exp} [*kN*]	$P_{ult} – P_{exp}$ [*kN*]	$(P_{ult} - P_{exp})/P_{ult}$ [%]
Diagonal anchorages – at an angle of 60° to the surface of the specimens						
1-L	165	13.5	4.21	4.7	-0.49	-11.6
2-R	165	13.5	3.78	4.1	-0.32	-8.5
3-L	165	13.5	8.62	9.3	-0.68	-7.9
4-R	165	13.5	6.09	5.8	0.29	4.8
5-L	165	13.5	6.52	2.9	3.62	55.5
6-R	165	13.5	6.09	4.9	1.19	19.5
7-L	165	13.5	4.21	7.6	-3.39	-80.5
8-R	165	13.5	9.22	10.6	-1.38	-15.0
Diagonal anchorages – at an angle of 90° to the surface of the specimens						
9-M	150	40	4.84	5.6	-0.76	-15.7
10-M	150	40	16.52	11.2	5.32	32.2
11-M	150	40	7.16	4.9	2.26	31.6
12-M	150	40	4.84	7.4	-2.56	-52.9

4 Comparison of the theoretical and experimental load-bearing capacity of anchors

A comparison of the load-bearing capacities of single anchors bonded perpendicular to the surface (Table 1) shows significant discrepancies between the values obtained from the experiment and those determined theoretically. In most cases, the theoretical load-bearing capacity is higher than the experimental load-bearing capacity (even by 79.0%). Four of the twenty-two tests found the opposite situation. In the case of anchors numbered 1, 5-6 and 17, the experimental load-bearing capacity (P_{exp}) was from 2.0% to even 139.5% higher than the theoretical load-bearing capacity (P_{ult}). In these cases, a higher class of concrete (C 30/37) and a resin with a lower adhesion stress value (τ_p = 5.89 N/mm^2) were used in the tested samples. It should be noted that during the experimental tests of single anchors bonded at an angle of 90° (Table 1), cracks in the thin structural layer with a thickness of 6 cm and splitting of the concrete around the anchorage zone were found in as many as 12 of the anchors. Such problems occurred in the case of anchors numbered: 3-4 (lower experimental load-bearing capacity than theoretical one by 69% and 52.3%, respectively), 7-8 (60.2%-66.1%), 10 (71.8%), 13-15 (57.9%-66.2%), 19-20 (72.0%-74.8%) and 22 (79.0%) and in anchor no. 17 – in which case the experimental load-bearing capacity exceeded the theoretical load-bearing capacity by as much as 139.5%.

A similar situation occurred with diagonally bonded anchors (Table 2). Only in the case of two tests (anchors nos. 3 and 9) the values of the experimental load-bearing capacity were higher than the theoretical load-bearing capacity – by 0.3% and 8.1%, respectively. In the remaining ten tests, the experimental load-bearing capacity of diagonal anchors was between 19.1% and 97.2% lower than the theoretical load-bearing capacity. The maximum discrepancies in the results were recorded for anchors numbered: 2 (71.9%), 5-6 (81.3% and 80.9%, respectively), 8 (85.3%), 10-

12 (97.2%, 58.3% and 72.0%, respectively). In these cases, uncontrollable factors were found, such as cracks in the structural layer slab and incomplete cleaning of the holes before anchoring. Significant discrepancies in the load-bearing capacity were also found in the case of anchor no. 7 (77.5%). However, its visual inspection after the examination did not show the influence of other, uncontrollable factors that could affect its load-bearing capacity.

A comparison of the theoretical and experimental load-bearing capacity in the case of two-anchor systems (Table 3) also shows large differences. Only in two cases (anchors nos. 14 and 16) higher values of the experimental load-bearing capacity were obtained than the theoretical load-bearing capacity (by 16.0% and 19.6%, respectively). In the remaining fourteen cases, the theoretical load-bearing capacity was higher than the experimental load-bearing capacity by 7.1% (anchor no. 15) to 93.6% (anchor no. 8). A partial justification for this fact is probably to be found, as before, in factors that could not be controlled during the experiment. Only six of the sixteen two-anchor systems (nos. 5, 10, 13-16) did not have problems with uncontrolled factors. In their case, the differences in experimental load-bearing capacity compared to the theoretical load-bearing capacity were much smaller and ranged from -35.8% to +19.6%. In the case of two-anchor systems, the short distance of the anchors from the edge (bonded at an angle of 30°) also had an additional adverse effect on the final experimental load-bearing capacity. Such a small distance of the anchors (about 5 *cm*) resulted from the adopted size of the samples of 40 × 20 *cm*.

The comparison of the load-bearing capacity of three-anchor systems (Table 4) is much better. In as many as seven tests, the experimental load-bearing capacity was higher than the theoretical load-bearing capacity (differences from 7.9% to 80.5%). Unfortunately, in five cases it was found that the experimental load-bearing capacity was lower than the experimental load-bearing capacity. The percentage decrease in the load-bearing capacity of P_{exp} in relation to P_{ult} is not as significant as in the case of single anchors and two-anchor systems and ranged from 4.8% (anchor no. 4) to 55.5% (anchor no. 5). The uncontrolled destruction mechanism in the group of three-anchor systems occurred only in the case of anchor no. 4 (right diagonal anchor).

5 Summary and conclusions

A comparison of the experimental load-bearing capacities (P_{exp}) with the corresponding theoretical load-bearing capacities (P_{ult}) of all the anchorages analyzed in the study shows very large discrepancies in the results, ranging from -97.2% to +139.5%. For single anchors bonded at a 90° angle to the specimen surface, the increase or decrease in P_{exp} value relative to P_{ult} is between -79.0% and +139.5%. For diagonal anchors, the load-bearing capacity ranged from -97.2% to +8.1%. In the case of two-anchor and three-anchor systems, the increases/decreases of the experimental load-bearing capacity in relation to the theoretical load-bearing capacity ranged from -93.6% to +19.6% and from -55.5% to +80.5%, respectively.

Obtaining, as a result of laboratory tests, higher values of experimental load-bearing capacities than theoretical ones is on the safe side. The optimal case would be to obtain P_{exp} several percentage points higher than P_{ult}. Unfortunately, in the case of the presented research, most of the results indicate the opposite tendency, in which the calculated theoretical load-bearing capacity exceeds (even significantly) the actual load-bearing capacity of the connections determined as part of the laboratory tests.

The relatively low experimental load-bearing capacity of some of the anchors tested compared to their theoretical ones may be due to factors that could not be controlled during the tests (such as cracks in the thin structural layer with a thickness of 6 cm). Taking into account the fact that a relatively low experimental load-bearing capacity compared to the theoretical load-bearing capacity was obtained in the case of most of the anchors tested, and only in some of the tests can the low values of P_{exp} be explained by uncontrollable factors or research errors, it should be concluded that it is necessary to undertake work aimed at developing new mathematical models/relationships that will better describe the actual nature of the anchors' work. These dependencies should include additional factors – including the-anchor mounting time and the time of setting. It also seems necessary to carry out additional tests of resin-to-steel and resin-to-concrete adhesion stresses.

The authors have attempted to do so using heuristic algorithms (genetic algorithm and local search algorithm). Detailed results of further work related to the development of new mathematical models, and their optimization and validation, will be presented in the next publication.

Bibliography

[1] Tomaszewicz D. Szlendak J. K. Jabłońska-Krysiewicz A. (2022): Oszacowanie teoretyczne nośności grup ukośnych kotew wklejanych na podstawie metody składnikowej. Materiały Budowlane. DOI: 10.15199/33.2022.10.04. No 10: 15-17.

[2] Grabowski K. (1908): „O przyczepności betonu do żelaza". Przegląd Techniczny. Tom XLVI. s. 521-522. Warszawa. 1908.

[3] Bryła St. (1937). O hakach w konstrukcjach żelazobetonowych. Przegląd Techniczny. Tom LXXVI. s.581-583. Warszawa.

[4] Cruz-Sena J. Cunha V. M. C. F. Camoes A. Barros J. A. O. Cruz P. (2009): Modelling of bond between galvanized steel rebars and concrete. Congreso de Metodos Numericos en Ingenieria 2009. Barcelona. 29 junio al 2 de junio 2009. s. 1-15. SEMNI. España 2009.

[5] Kijania M. (2015). Metody wyznaczania wartości naprężenia przyczepności pomiędzy betonem a stalą zbrojeniową. Przegląd Budowlany 6/2015. s. 38-42.

[6] Smarzewski P., Stolarski A. (2007). Badanie i wyznaczanie naprężeń przyczepności betonu do stali zbrojeniowej". Biuletyn WAT. Vol. LVI. Nr 1. 2007. s. 7-24.

[7] Słowik M., Błazik-Borowa E. (2001). Wpływ doboru prętów zbrojeniowych na rozkład naprężeń w elemencie betonowym. Eksploatacja i Niezawodność nr 5/2001. s. 43-46.

[8] Tomaszewicz D., Baryłka A. (2020). Wpływ kształtu powierzchniowego kotew wklejanych na ich nośność – Materiały Budowlane 6/2020, 52-53

[9] Szlendak J. K. Jabłońska-Krysiewicz A. Tomaszewicz D. (2018). Assessment of the load capacity of the anchorage system connecting the textured layer with the structural wall of large slab buildings in the lights of experimental research and FEM analysis – *3rd Scientific Conference Environmental Challenges in Civil Engineering (ECCE 2018).* MATEC Web of Conferences 174. Article Number 03016. Section Design of Buildings. Including Reconstruction and Renovation of Antique Buildings (2018). 697-707. Opole 23÷25.04.2018

[10] Tomaszewicz D. (2023). *Badanie interakcyjnej nośności kotew mocujących warstwę fakturową do warstwy konstrukcyjnej w budownictwie wielkopłytowym*. [Rozprawa doktorska – Promotor: prof. dr hab. inż. Jerzy Kazimierz Szlendak]

[11] CEN/TS 1992-4-1:2009 „Design of fastenings for use in concrete. Part 4-1: General"

[12] Model Code for Concrete Structures. CEB Bulletin d'Information No195 and 196, First Draft, March 1990.

[13] PN-EN 1992-1-1. Eurokod 2 „Projektowanie konstrukcji z betonu. Część 1-1: Reguły ogólne i reguły dla budynków."

[14] Baryłka A., Tomaszewicz D. Relationship of the interaction load capacity of anchors on their number and anchoring system. *Archives of Materials Science and Engineering, Volume 112: Issue 2,* 55-62, ORCID identifier: https://orcid.org/0000-0002-0181-6226 (A.B.); https://orcid.org/0000-0002-1359-902X (D.T.) DOI: 10.5604/01.3001.0015.6286